Experimental demonstration of bindingless signal delivery in human cells via microfluidics

Ching-Te Kuo, Fang-Tzu Chuang, Pei-Yi Wu, Yueh-Chien Lin, Hao-Kai Liu, Guan-Syuan Huang, Tzu-Ching Tsai , Cheng-Yu Chi, Andrew M. Wo, Hsinyu Lee, and Si-Chen Lee

Citation: Journal of Applied Physics **116**, 044702 (2014); doi: 10.1063/1.4891017
View online: http://dx.doi.org/10.1063/1.4891017
View Table of Contents: http://scitation.aip.org/content/aip/journal/jap/116/4?ver=pdfcov
Published by the AIP Publishing

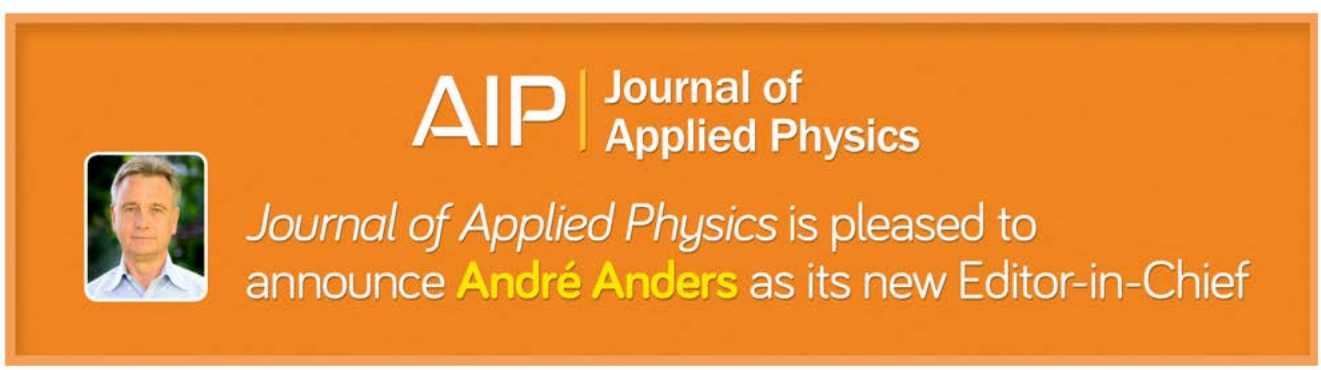

Experimental demonstration of *bindingless* signal delivery in human cells *via* microfluidics

Ching-Te Kuo,[1,2,a)] Fang-Tzu Chuang,[3,a)] Pei-Yi Wu,[4,a)] Yueh-Chien Lin,[4] Hao-Kai Liu,[1] Guan-Syuan Huang,[1] Tzu-Ching Tsai,[4] Cheng-Yu Chi,[3] Andrew M. Wo,[1] Hsinyu Lee,[4,b)] and Si-Chen Lee[3,c)]

[1]*Institute of Applied Mechanics, National Taiwan University, Taipei, Taiwan*
[2]*Institute of Atomic and Molecular Sciences, Academia Sinica, Taipei, Taiwan*
[3]*Department of Electrical Engineering, Graduate Institute of Electronics Engineering, National Taiwan University, Taipei, Taiwan*
[4]*Department of Life Science, National Taiwan University, Taipei, Taiwan*

(Received 25 February 2014; accepted 12 July 2014; published online 23 July 2014)

The cellular signal transduction is commonly believed to rely on the direct "contact" or "binding" of the participating molecule reaction that depends positively on the corresponding molecule concentrations. In living systems, however, it is somewhat difficult to precisely match the corresponding rapid "binding," depending on the probability of molecular collision, existing in the cellular receptor-ligand interactions. Thus, a question arises that if there is another mechanism (i.e., *bindingless*) that could promote this signal communication. According to this hypothesis, we report a cellular model based on the examination of intracellular calcium concentration to explore whether the unidentified signal delivery in cells exists, *via* a microfluidic device. This device was designed to isolate the cells from directly contacting with the corresponding ligands/molecules by the particular polydimethylsiloxane (PDMS) membranes with different thicknesses. Results show a significant increment of calcium mobilization in human prostate cancer PC-3 cells by the stimulation of endothelin-1, even up to a separated distance of 95 μm. In addition, these stimulated signals exhibited a bump-shaped characteristics depending on the membrane thickness. When the PDMS membrane is capped by SiO_2, a particular trait that resembles the ballistic signal conduction was observed. A theoretical model was developed to describe the signal transport process across the PDMS membrane. Taken together, these results indicate that the unidentified signal (ligand structural information) delivery could occur in cells and be examined by the proposed approach, exhibiting a *bindingless* communication manner. Moreover, this approach and our finding may offer new opportunities to establish a robust and cost-effective platform for the study of cellular biology and new drug development. © *2014 AIP Publishing LLC*. [http://dx.doi.org/10.1063/1.4891017]

I. INTRODUCTION

For hormone triggered cellular functions, ligands were suggested to bind directly with specific receptors to induce downstream signals. The relationship between ligand and its receptor is proposed as the relationship between lock and key. In a suspension system, the possibility for a tumbling key to hit the lock in a perfect position and unlock it may be extremely low as illustrated in Figure 1(a). Similarly, a perfect match between ligands and receptors in the cell system may encounter a similar situation. Therefore, we hypothesized that direct binding may not be necessary for the receptor activation. That is, ligands might release signals related to structural information automatically when they hit the cell membrane in a binding independent manner and activate receptors without direct binding (Figure 1(a)).

Herein, we present an experimental approach *via* microfluidic devices to demonstrate that the cell-molecule interaction could exist in a binding independent manner. We use endothelin (ET) as a ligand, which can activate human prostate cancer PC-3 cells and subsequently mobilization intracellular calcium rapidly. The system can be monitored by calcium assay with loading the cells with fluorescent Fluo-2 dyes that binds to free intracellular calcium, and enhanced fluorescence signals after treatment with endothelin-1 (ET-1).[1,2] The microfluidic device contains two perpendicular microchannels sandwiching a customized membrane that supports cells, which can isolate cells from direct binding with the corresponding molecules (Figure 1(b)). Therefore, the *bindingless* signal delivery—ET-1 ligands to ET receptors interaction—could be explored experimentally. Taken together, the proposed approach have advantages of viable culture of cellular microenvironment and study of *bindingless* signal delivery between cells and molecules, which may be further applicable for new drug developments and biological assays.

II. MATERIALS AND METHODS

A. Fabrication of the microfluidic device

Fabrication began with alignment and permanent bonding of two microchannels and a customized membrane with

[a)]Ching-Te Kuo, Fang-Tzu Chuang, and Pei-Yi Wu contributed equally to this work.
[b)]E-mail: hsinyu@ntu.edu.tw
[c)]E-mail: sclee@ntu.edu.tw

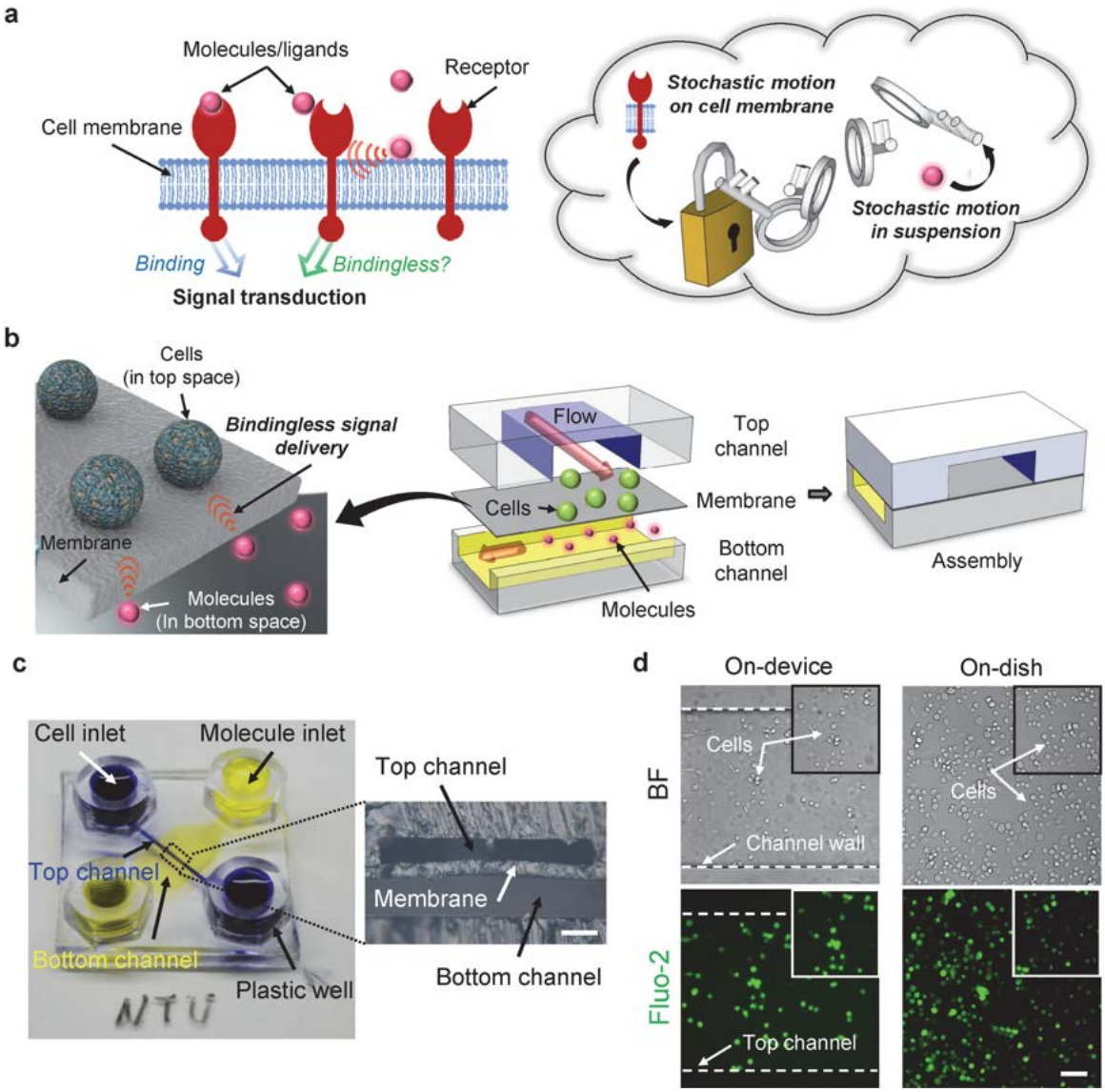

FIG. 1. Design of a microfluidic device for the demonstration of *bindingless* signal delivery in cells. (a) Depiction of traditional (contact) and unidentified signal transductions between cells and the corresponding molecules/ligands. (b) Illustration of the overall device configuration with top and bottom channels sandwiching the cell-supporting membrane that isolated cells and molecules. (c) Photography of the fabricated device in which four wells were used as reservoirs to control the flow rates by selectively tuning the solution levels. Blue and yellow colors represented the top and bottom channels, respectively. Blue wells were served as the cell inlet/outlet, and yellow ones served as the molecule inlet/outlet. The enlarged image shows the cross-sectional view of the three-layered device. (d) Results obtained with on-device cell culture by PC-3 cells stained with Fluo-2 dyes, and those obtained with on-dish culture. Scale bars, 100 μm.

various thicknesses as shown in Figure 1(b). The top and bottom channels were fabricated by casting polydimethylsiloxane (PDMS) (sylgard 184, Dow Corning) prepolymer against two photoresist-made (THB-151N, JSR) masters that contain two positive reliefs of orthogonal microchannels. The dimensional size was 600-μm width $\times$ 85-μm height for the top channel and 8000-μm width $\times$ 40-μm height for the bottom channel. Slender posts, with a width of 50 μm and separated by 1100 μm, were designed on the bottom channel to prevent the collapse between the two channels. Holes of 1 mm in diameter were mechanically drilled through the cured channels, acting as fluidic inlet/outlet connections. The membrane was fabricated by spin-coating PDMS prepolymer (10:1) on a flat glass substrate. The thicknesses of the membranes were 10, 20, 35, 50, and 95 μm by spin-coating individually at 2500 rpm for 120, 60, 30, 20, and 10 s. After curing at 70 °C for 1 h, the top channel was aligned and bonded with the membrane by oxygen plasma treatment (30 sccm, 60 W, 60 s). Subsequently, the bottom surface of the membrane was treated with oxygen plasma and bonded to the bottom channel. PMMA nuts (5 mm in both diameter and height; inner volume of $\sim$100 μl) were used as solution reservoirs and adhered onto the inlet/outlet holes of the device *via* PDMS prepolymer cured at 70 °C for 1 h to achieve irreversible bonding. To further confirm the inhibition of small molecules permeating through the membrane, we modified the membrane surface with 60-nm SiO_2 by double-site-deposition using electron beam evaporation (ULVAC). Figure 1(c) shows the top features of the microdevice containing four wells. The blue wells served as the inlet/outlet for the top channel, and the yellow ones as the condition sink for the bottom channel.

B. Cross-sectional characterization of the membrane using SEM and TEM

For membrane surface characterization monitoring by scanning electron microscope (SEM; ERA-8800FE) and transmission electron microscope (TEM; JEOL 2100 F), a cross-sectional specimen of the membrane was examined. Furthermore, low angle annular dark field (LAADF) TEM images were utilized to examine voids inside the membrane and coated SiO_2 as described.[3]

C. Cell culture

PC-3 cell line (CRL-1435, ATCC) was maintained in RPMI-1640 medium (23400–021, GIBCO), supplemented with 10% fetal bovine serum (FBS, SV30014, Hyclone) and 1% penicillin/streptomycin (15140, GIBCO) in a humidified 5% CO_2 incubator at 37 °C.

D. ET-model experiment

Prior to loading of cells, the microfluidic device was first sterilized by UV light in a laminar-flow hood overnight. The device was then placed in the vacuum chamber to degas for 10 min, followed by filling with 70% ethanol. Afterwards, the device was washed twice with phosphate buffered saline (PBS) and stored in a sterilized dish by sealing with parafilm at 4 °C until needed.

For ET-model experiment, type I collagen solution (BD Biosciences; 100 μg/ml in PBS) was loaded into the top channel and placed in a humidified incubator at 37 °C for 1 h to allow binding to the membrane. Then, PBS and culture medium were introduced to wash away unbound collagen. 100 μl of PC-3 cells ($\sim 1.5 \times 10^3$ cells) in culture medium were loaded into the top channel by tuning the solution level height as described.[4] Afterward, the solution heights were kept the same to enable cell attachment and spread on the membrane in a 5% CO_2 incubator at 37 °C overnight. Subsequently, Fluo-2 AM fluorescent dye (0210, Teflabs) was introduced into the top channel to stain cells for 1 h. Afterward, fresh medium was perfused to wash away residual dyes. ET-1 (SI-E7764-50UG, SIGMA) was then introduced into the top or bottom channel, served as control or experimental set, respectively. The resulted fluorescence was captured by a charge-coupled device (CCD) camera (DP-70, Olympus) on an inverted microscopy and the fluorescent intensity was determined by using an imaging software (ImageJ, 1.42q).

E. Statistical analysis

Student's t test was used to compare data from two groups of data, and ANOVA test was used to compare data from more than two groups. ($p < 0.05$ was considered statistical significant).

III. RESULTS AND DISCUSSION

The efficacy of the microdevice (Figure 1(c)) in enabling *in-vitro* cell culture (Figure 1(d)), the characterization and permeation testing of the fabricated membrane, and the subsequent demonstration of *bindingless* signal delivery between cell receptors and their corresponding ligands/molecules from ET model will be presented below. Additional information is also available in the Supplementary Material.

A. Cross-sectional characterization and permeation test of the PDMS membrane

The hydrophobic nature of PDMS tends to adsorb small hydrophobic molecules and proteins although the limit molecular permeation into PDMS is in the $100 \sim 300$ molecular weight (MW) range.[5–7] To further confirm whether the ET-1 ligands (MW = 2492) can permeate into the PDMS membrane, we conducted two approaches to verify it. First, Figure 2(a) shows the SEM and LAADF TEM images of the membrane, both surfaces were coated with a 60-nm SiO_2 layer. The purpose of this surface modification is to effectively prevent the molecular permeation and acquire hydrophilic wall characteristics, as described.[8] There is no apparent void within the PDMS and SiO_2 layers among the observation zone, even examined from higher resolution TEM images, i.e., no voids larger than 10 nm were detected (data not shown). Second, Figure 2(b) shows the permeation testing by using small molecule nuclei dyes (Hoechst 33342; MW = 616), which were loaded from the bottom channel of the microdevice. Results obtained from the P-control revealed that apparent nuclei signals were detected and significantly increased depending on the dye concentration, whereas no significant difference was examined between the experimental sets (Figure 2(c)). In addition, the nuclei signals from the experimental sets were significantly lower than the P-control but corresponding to the background signal, even from different membrane thicknesses (Figure S1).[9] Therefore, these findings suggest that large molecules, e.g., ET-1, cannot permeate into the PDMS membrane from the bottom channel to the top, indicating that the proposed ET model can be adopted for the following demonstration.

B. Demonstration of *bindingless* signal delivery in ET model

To explore whether an unidentified signal delivery pathway exists in the cellular receptor-ligand interaction afforded by *binding*, we followed the procedure (ET model) illustrated in Figure 3(a) to examine this phenomenon (details can refer to the MATERIALS AND METHODS). Several results are noteworthy. First, cells cultured on the PDMS membranes (either with or without SiO_2 modification) all acquired a significant upregulation of fluorescent intensity compared to the N-control, whereas these upregulations were lower than that of the P-control at the 5-min time point (Figures 3(b) and 3(c)). In addition, a significant downregulation of intensity in the N-control was examined at 5 min (Figure 3(b)), suggesting that photobleaching of the fluorescent dyes could dominate it as others reported.[10,11] Note that the signal responses at the 10-min time point behaved the corresponding traits as well (please see the time-lapse results as shown in Figure S2).[9] Second, the signal intensity of cells, after the ET-1 stimulation, versus different membrane thicknesses displayed a bump-shaped characteristics for PDMS

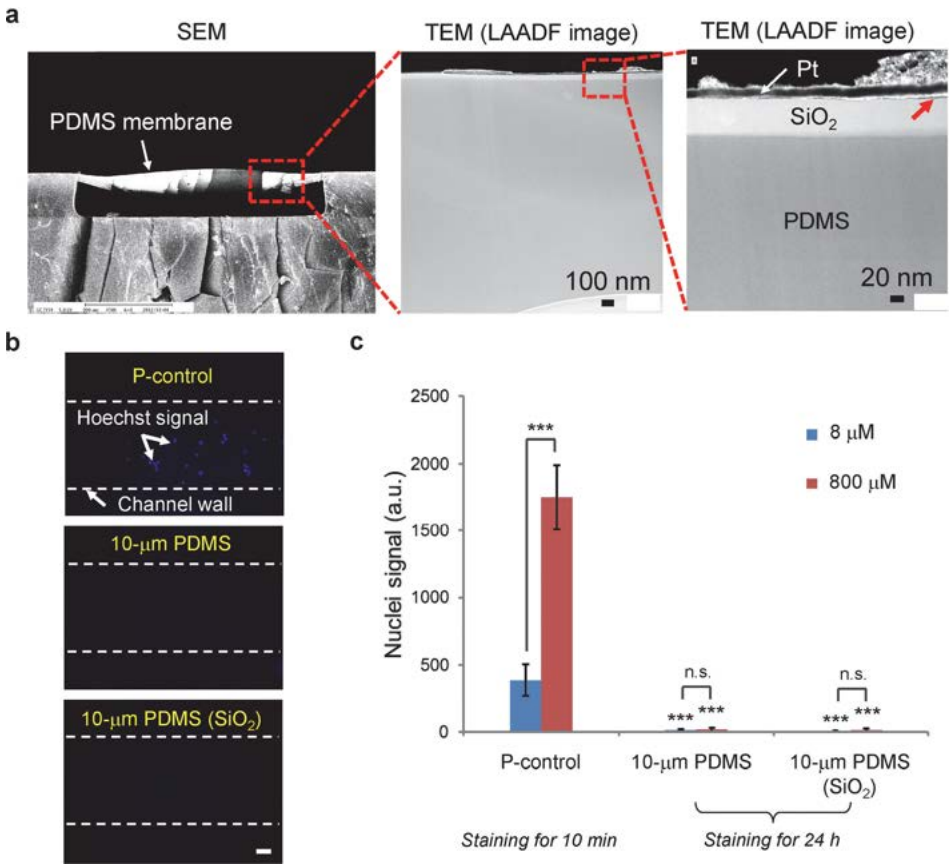

FIG. 2. Cross-sectional characterization and permeation testing of the fabricated membrane. (a) SEM and LAADF TEM images of the membrane. The red arrow indicated the void (~2 nm) between the Pt and SiO_2. (b) Permeation testing of the membrane by loading with Hoechst 33342 nuclei dyes. P-control indicated that nuclei dyes were loaded from the top channel. In contrast, the others indicate that dyes were from the bottom channel. Scale bar, 100 μm. (c) Total area of Hoechst (with concentrations of 8 μM and 800 μM) signal intensities in cells were measured. P-control was stained for 10 min, whereas the others were for 24 h. Each bar represents the mean ± SD (n = 9 ~ 49 cells), ***p < 0.001 compared to P-control (for 8 μM and 800 μM, respectively), except for the indicators.

with and without SiO_2 deposition (Figures 3(d) and 3(e)). In bare PDMS membrane cases, the intensity increased linearly for $d < 35$ μm, whereas it decreased linearly depending on the thickness for $d > 35$ μm (Figure 3(d)). The highest response was achieved in the 35-μm PDMS and the lowest one was in the 95-μm PDMS. No significant difference was detected in the 20- and 50-μm PDMS compared to the 10-μm PDMS. For PDMS membrane coated with SiO_2, the behavior is similar at $d < 35$ μm but change very little for $d > 35$ μm (Figure 3(e)), suggesting that the surface modification by SiO_2 could increase the signal delivery distance. The highest intensity stimulated was achieved in the 20-μm PDMS, whereas no significant difference was detected in the rest membranes. Third, the resulted intensity was dependent on the molecular concentration adapted (Figure 3(f)). Note that the intensity was downregulated near to the background for a higher ET-1 concentration (5 μM). For lower concentrations (0.1 μM and 2 μM ET-1), however, they acquired a significant increment of intensity. These findings indicate that a *bindingless* signal delivery may exist between cellular receptors and ligands, and it could be examined by this ET model.

For conventional dose-response drugs/molecules treatment, most the effects are dependent on the concentration of the active ingredient in cells, e.g., drugs with higher concentrations would cause more profound effects on cells than those of the lower concentrations.[5,12] Furthermore, other research group had revealed that the stimulated intracellular calcium concentration is positively dependent on the corresponding molecule concentration,[13] which is consistent with our on-device P-control (i.e., binding signal delivery) experiments (Figure S3).[9] However, it is somewhat not consistent in micro/nano-scaled applications. For example, nanoworms linked by targeted ligands with a high concentration may not achieve a more effective tumor-targeting efficiency than with a low concentration.[14] In addition, our results show that the intracellular calcium concentration, which is proportional to the fluorescent intensity in cells, acquired a higher increment under the stimulation of low ET-1 concentration rather than with high concentration as well (Figure 3(f)). These suggest that the *bindingless* signal delivery (i.e., cellular receptor-ligand *contactless* communication) behaves an effective way under the low ligand concentration regime in micro/nano scales. However, it has the possibility that the high ET-1 concentration of 5 μM utilized in this work stimulates a higher and faster response which might return to the base line at 5 min, thus questioning our assumption above. Therefore, further studies will be needed to examine this statement. Furthermore, the molecular diffusion/permeation depends on the mechanism of which molecules from high to low concentration. In other words, the stimulated intensity by high ET-1 concentration in the ET model should be larger than that by low concentration if the permeation dominates. However, due to the distinct results (comparing with 0.1 μM and 2 μM ET-1 in Figure 3(f)), the permeation of ET-1 molecules into the PDMS membrane to the top cell-supporting channel might not exist, thus confirming our hypothesis in this work.

C. Physical characteristics of the *bindingless* signal delivery

To explore the particular physical attributes afforded by the *bindingless* signal delivery revealed above, we

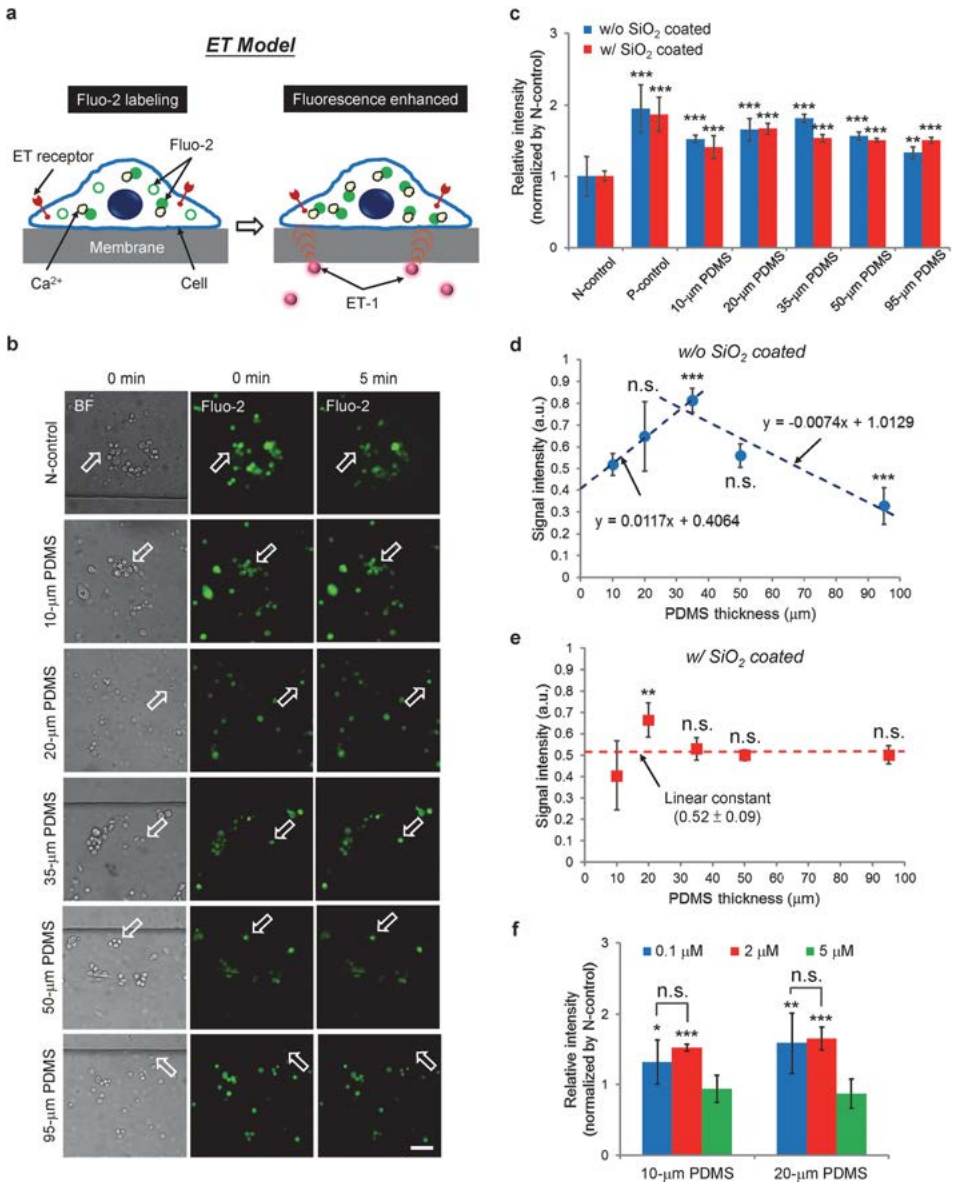

FIG. 3. *Bindingless* signal delivery between cells and the corresponding molecules. (a) Depiction of the ET model utilized for the demonstration of *bindingless* interaction between ET receptors and ET-1 ligands in the microfluidic device. (b) Time sequence of the top-viewed photographs showing Fluo-2 dye-stained PC-3 cells in the top channel under the 2 μM ET-1 stimulation from the bottom channel. ET-1 was loaded at the 0 min. N-control indicated that no ET-1 was applied. The thicknesses of the membranes tested were from 10 ~ 95 μm. The largest differentiation on the fluorescent intensity in cells was highlighted by the empty arrows. Scale bar, 100 μm. (c) Total area of Fluo-2 signal intensities in cells were measured by Image J software at the 5 min. The relative intensity was normalized by the N-control. P-control indicated that ET-1 was loaded from the top channel. The membranes used were bare PDMS (w/o SiO_2 coated) and pretreated PDMS (w/ SiO_2 coated), respectively. (d) and (e) show the signal intensity versus different membrane thicknesses (bare and pretreated PDMS, respectively). The intensity was defined as the relative intensity from (c) subtracted the background signal (N-control). (f) The relative intensity measured at the 5 min versus different ET-1 concentrations. Each data represent the mean ± SEM from 2 ~ 4 independent experiments (n = 50 ~ 134 cells). *p < 0.05, **p < 0.01, and ***p < 0.001 were compared to the N-control in (c) (for w/o and w/ SiO_2 coated, respectively), the 10-μm PDMS in (d) and (e), and the 5 μM ET-1 in (f), except for the indicators.

developed a physical model to describe this phenomenon (Figure 4(a)). First, we assumed that the effective capture cross section of a ligand that docks on the back surface of PDMS membrane is A, which is perpendicular to the PDMS surface. The structure information A could propagate to the top surface of the membrane and result in a cone shape with a half angle θ. The total volume of the structure information (capture cross section σ) from the ligand A, which can stimulate cells on the top surface of the membrane, thereby turns out to be

$$\sigma = 2\pi d \tan\theta A, \tag{1}$$

where d is the thickness of the membrane. Second, this structure information may be distorted or scattered by the disordered membrane or other nearby cone structure information, thus resulting in a mean free path l for the signal delivery, therefore, the modified capture cross section σ is given by

$$\sigma = 2\pi d \tan\theta A e^{-\frac{d}{l\cos\theta}}. \tag{2}$$

Third, we assumed that the enhanced signal intensity f of cells stimulated by ET-1 ligands is corresponding to the capture cross section σ, thereby the intensity f can be given by

$$f \equiv c\sigma = c2\pi d \tan\theta A e^{-\frac{d}{l\cos\theta}} = axe^{-x}, \tag{3}$$

where c is a constant, $a = 2\pi l \sin\theta\, c\, A$ is a scaling factor determined by surface roughness and material property of the membrane, and $x = d/l\cos\theta$. The material properties of the membrane may affect the tilted angle θ of the cones and the resulted interactions among the tilted cones tend to distort and scatter the structure information of ligands and then degrade the mean free path l.

From Eq. (3), it is clear that when membrane thickness is much lower than the mean free path, the resulted signal intensity of cells would be linearly dependent on the membrane thickness and then decay at a larger thickness, showing a bump-shaped curve as illustrated in Figures 3(d) and 3(e). Figures 4(b) and 4(c) show the comparisons of the theoretical model, fitted from Eq. (3), with the experimental

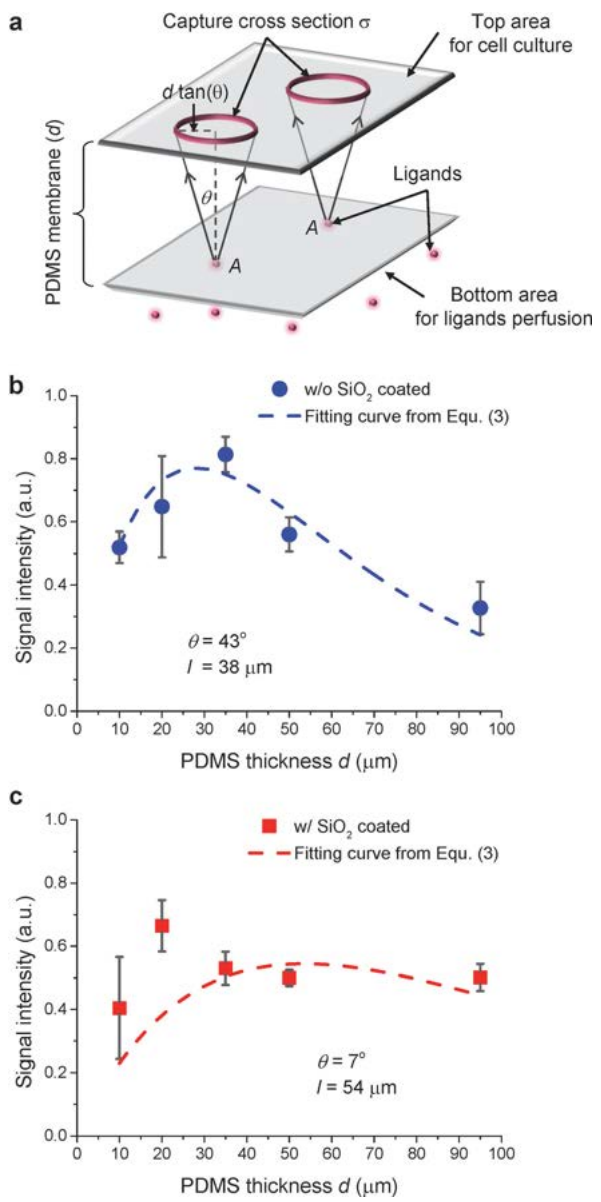

FIG. 4. Model of the *bindingless* signal delivery. (a) A schematic diagram of this signal delivery from the structure information A of ligands in bottom area to the top (cell culture region) of the PDMS membrane. Here, A is the effective capture cross section of a ligand that docks on the bottom PDMS surface, σ is the total volume of the structure information that can stimulate cells on the top PDMS surface, θ is the half angel of the cone shape resulted from A, and d is the thickness of the membrane. (b) and (c) show the experimental results from Figures 3(d) and 3(e), respectively, and the correspondingly fitted curves from Eq. (3).

results from Figures 3(d) and 3(e). The fitted tilt angle θ of cones and mean free path l were 43° and 38 μm for bare PDMS, 7° and 54 μm for SiO_2-coated PDMS. The fitting trend was similar by using bare PDMS but did not exactly match by pretreated PDMS at thinner thickness $d < 30$ μm, indicating that the surface modification by SiO_2 might cause an additional effect on the signal delivery. For bare PDMS, the rough membrane surface may cause tilted cones that interact with each other and degrade the mean free path to 38 μm (Figure 4(b)). However, for SiO_2-coated PDMS (Figure 4(c)), the structure information behaved with a longer mean free path (54 μm), a ballistic signal transduction without energy dissipation (no exponential decay term) may exist at thinner membrane thickness $d < 35$ μm that led to higher signal intensity than theory.

The surface characteristic of the SiO_2-coated PDMS was examined by AFM imaging as shown in Figure S4,[9] which revealed that curvilinear micro/nano structures can be achieved with a uniform wavelength of $4 \sim 5$ μm and a amplitude of 400 nm. These structures may be caused by the buckling of thin SiO_2 films due to thermal contraction of the PDMS substrate, as other reported by metal films on PDMS.[15] In addition, several reports have revealed that omnidirectionally arranged curvilinear surfaces inspired from biological compound eyes may improve the signal detection and sensitivity.[16,17] Indeed, we examined the concentrated tilt angle of cones (from 43° to 7°) and the enhanced mean free path of the signal delivery (from 38 to 54 μm) by the modified PDMS compared to the bare one as well. Based on this observation, we suggest that this curvilinear surfaces on the SiO_2-coated PDMS may improve the *bindingless* signal delivery passing through the PDMS membrane.

Notably, the above results behave somewhat like a phonon conduction in micro/nano or ordered polymer structures,[18–20] which revealed the unconventional thermal (signal) transduction, i.e., the signal intensity is a constant independent of the thickness. However, the theoretical model defined herein is not optimized but should be considered including other parameters (e.g., ligand/receptor/material properties, temperature, time, etc.) in the future study.

IV. CONCLUSIONS

In summary, we have presented a microfluidic device and a cellular model for the demonstration of *bindingless* signal delivery between the cellular receptors and molecules, which were isolated by a customized PDMS membrane. This strongly suggests that the real biochemical interaction could take place upon a ligand hit the cell membrane where the receptors are embedded in, indicating that the direct binding between ligand/receptor is unnecessary. Toward this end, surface characteristic examination and permeation testing were utilized to confirm the membrane performance. Key results demonstrated that the *bindingless* signal delivery in cells could occur by the proposed ET model examination. Furthermore, the physical characteristics of the signal delivery somewhat resembled the diffusive and ballistic thermal conductions in micro/nano scales.[19] These findings in this work could provide a proof-of-conception demonstration of the unidentified signal delivery (i.e., "X" signal) in living systems and may be used for a range of applications in drug development and biological research.

ACKNOWLEDGMENTS

The authors would like to thank President Yin for financially supporting this research under Contract No. FR001-2.

[1]D. M. Pollock, T. L. Keith, and R. F. Highsmith, FASEB J. **9**, 1196–1204 (1995).
[2]W. J. Wasilenko, J. Cooper, A. J. Palad, K. D. Somers, P. F. Blackmore, J. S. Rhim, G. L. Wright, Jr., and P. F. Schellhammer, Prostate **30**, 167–173 (1997).

[3]A. Kovacs, J. Sadowski, T. Kasama, M. Duchamp, and R. E. Dunin-Borkowski, J. Phys. D: Appl. Phys. **46**, 145309 (2013).
[4]C.-T. Kuo, C.-L. Chiang, Ruby Y.-J. Huang, H. Lee, and A. M. Wo, NPG Asia Mater. **4**, e27 (2012).
[5]L.-C. Hsiung, C.-L. Chiang, C.-H. Wang, Y.-H. Huang, C.-T. Kuo, J.-Y. Cheng, C.-H. Lin, V. Wu, H.-Y. Chou, D.-S. Jong, H. Lee, and A. M. Wo, Lab Chip **11**, 2333–2342 (2011).
[6]K. Ozasa, J. Lee, S. Song, M. Hara, and M. Maeda, Lab Chip **13**, 4033–4039 (2013).
[7]M. W. Toepke and D. J. Beebe, Lab Chip **6**, 1484–1486 (2006).
[8]G. T. Roman, T. Hlaus, K. J. Bass, T. G. Seelhammer, and C. T. Culbertson, Anal. Chem. **77**, 1414–1422 (2005).
[9]See supplementary material at http://dx.doi.org/10.1063/1.4891017 for four images showing the permeation testing with different membrane thicknesses (Figure S1), the time-sequenced responses of the signal intensities (Figure S2), the relative intensity of postive control versus ligand concentrations (Figure S3), and the surface characteristics of the pretreated PDMS (Figure S4).
[10]C. Mayer, J. Wachtler, M. Kamleiter, and P. Grafe, Neurosci. Lett. **224**, 49–52 (1997).
[11]J. H. Hong, C. H. Min, B. Jeong, T. Kojiya, E. Morioka, T. Naqai, M. Ikeda, and K. J. Lee, PLoS One **5**, e9634 (2010).
[12]C.-T. Kuo, C.-L. Chiang, C.-H. Chang, H.-K. Liu, G.-S. Huang, R. Y.-J. Huang, H. Lee, C.-S. Huang, and A. M. Wo, Biomaterials **35**, 1562–1571 (2014).
[13]C.-Y. Pan, H. Lee, and C. L. Chen, Neuropharmacology **51**, 18–26 (2006).
[14]J.-H. Park, G. von Maltzahn, L. Zhang, A. M. Derfus, D. Simberg, T. J. Harris, E. Ruoslahti, S. N. Bhatia, and M. J. Sailor, Small **5**, 694–700 (2009).
[15]N. Bowden, S. Brittain, A. G. Evans, J. W. Hutchinson, and G. M. Whitesides, Nature **393**, 146–149 (1998).
[16]L. P. Lee and R. Szema, Science **310**, 1148–1150 (2005).
[17]K.-H. Jeong, J. Kim, and L. P. Lee, Science **312**, 557–561 (2006).
[18]M. E. Siemens, Q. Li, R. Yang, K. A. Nelson, E. H. Anderson, M. M. Murnane, and H. C. Kapteyn, Nature Mater. **9**, 26–30 (2010).
[19]T. K. Hsiao, H. K. Chang, S. C. Liou, M. W. Chu, S. C. Lee, and C. W. Chang, Nat. Nanotechnol. **8**, 534–538 (2013).
[20]J.-H. Lee, C. Y. Koh, J. P. Singer, S.-J. Jeon, M. Maldovan, O. Stein, and E. L. Thomas, Adv. Mater. **26**, 532–569 (2014).